Biological Control 206 (2025) 105790

Contents lists available at ScienceDirect

Biological Control

journal homepage: www.elsevier.com/locate/ybcon

Whole genome analysis of antagonistic and plant growth promoting *Bacillus halotolerans* KFD uncovers its molecular arsenal against the bayoud pathogen *Fusarium oxysporum* f.sp *albedinis*

Aliou Moussa Diouf[a,*], Abdou Lahat Mbaye[a], Maimouna Deh[a], Mustapha Barakate[a,b,*], Zineb Rchiad[c,*]

[a] College of Agriculture and Environmental Sciences, Plant Pathology Program, Agrobiosciences, Mohammed VI Polytechnic University (UM6P), Ben Guerir, Morocco
[b] Cadi Ayyad University (UCA), Faculty of Sciences-Semlalia, Laboratory of Water Sciences, Microbial Biotechnologies, and Natural Resources Sustainability (AQUABIOTECH), Unit of Microbial Biotechnologies, Agrosciences, and Environment (BIOMAGE)-CNRST Labeled Research Unit N 4, PO Box 2390, Marrakesh 40000, Morocco
[c] Biosciences CoreLab, Mohammed VI Polytechnic University (UM6P), Ben Guerir, Morocco

HIGHLIGHTS

- Identification of novel Bacillus halotolerans strain with biocontrol activities.
- The strain showed high antifungal activities against different fungal pathogens.
- The strain showed protective effect on date palm against the bayoud disease.
- Comparative genomics showed that the strain harbored unique antifungal genes.
- First report of Bacillus halotolerans biocontrol agents isolated from date palm.

ARTICLE INFO

Keywords:
Biocontrol agents
Date palm
Fusarium oxysporum f.sp. *albedinis*
Bayoud disease
Bacillus halotolerans
Antifungal
Genome analysis
PGPR

ABSTRACT

The bayoud disease stands as a serious threat to date palm cultivation and production in North Africa, particularly in Morocco. Biocontrol agents constitute an eco-friendly alternative solution to this problem, as breeding techniques or the use of chemical pesticides did not yield promising results, leading farmers to burn infected trees to limit the pathogen propagation. In this frame, we screened different bacteria isolated from date palm root surface for their potential to inhibit the pathogen *F. oxysporum* f.sp. *albedinis* (Foa). Out of forty tested isolates, one isolate showed promising results against Foa and exhibited as well broad-spectrum antifungal properties. Moreover, this isolate showed plant growth promotion (PGP) traits. We also conducted a greenhouse assay to evaluate the protective effect of our isolate. The result showed that our isolate effectively protected date palm seedlings against Foa. The genome characterization showed that our isolate has a genome size of approximately 3.9 MB and belongs to *Bacillus halotolerans*. We annotated 11 secondary metabolite gene clusters encompassing six known antifungal clusters, namely bacillibactin, bacilysin, bacillaene, fengycin, surfactin, and plipastatin. Moreover, we identified genes that encode carbohydrate-active enzymes involved in chitinase activities as well as the degradation of glucan in fungal cell walls. The screening of genes linked to plant growth promotion identified genes involved in phosphate metabolism, indole-3-acetic acid and siderophore production, and free nitrogen fixation.

Our results show that *B. halotolerans* KFD represents a potential biocontrol agent that could be used to manage bayoud disease and promote the growth of date palm. To the best of our knowledge, our study is the first to isolate and decipher the genomic features of a *B. halotolerans* strain from the rhizosphere of date palm.

* Corresponding authors at: Mohamed VI Polytechnic University, Ben Guerir 43150, Morocco.
E-mail addresses: diouf.moussa@um6p.ma (A.M. Diouf), mustapha.barakate@um6p.ma (M. Barakate), zineb.rchiad@um6p.ma (Z. Rchiad).

https://doi.org/10.1016/j.biocontrol.2025.105790
Received 26 February 2025; Received in revised form 6 May 2025; Accepted 6 May 2025
Available online 10 May 2025

1. Introduction

Bayoud disease, also known as Palm Dieback, is a devastating fungal disease caused by *Fusarium oxysporum* f. sp. *albedinis* (Foa). Historically, bayoud disease has inflicted severe damage on date palm plantations, particularly in North Africa (El Modafar, 2010). This disease poses a significant threat to date palm production because of its rapid spread and the lack of efficient management techniques where farmers usually burn infected trees to limit the pathogen propagation (Rafiqi et al., 2022). Bayoud disease initially manifests with the browning of one side of infected leaves, from the base to the top, and is generally observed on the leaves of the middle crown. Afterwards the infection spreads on the other side of the leaves from the top to the base progressing to the entire canopy's decline and causing the eventual death of the plant. Recent *in silico* analyses of the Foa genome showed that it harbors genes that encode effector proteins thought to be involved in pathogenicity (Rafiqi et al., 2022). However, the infection mechanisms of the pathogen and the *in vivo* study of the predicted effectors remain to be elucidated. Understanding the infection mechanisms could consolidate efforts on integrated disease management research.

The use of antagonistic microbial organisms could constitute a promising approach to control the propagation of bayoud disease, as microorganisms have been widely used in agriculture to manage plant diseases. These micro-organisms, referred to as biocontrol agents (BCAs), employ different mechanisms to limit pathogen infections and protect plants (Ghorbanpour et al., 2018; Köhl et al., 2019). Bacteria belonging to the genus *Bacillus* have been reported to control different phytopathogens (Correa and Soria, 2010; Shafi et al., 2017) and are considered one of the most effective classes of BCAs. Bacteria belonging to this genus can produce different secondary metabolites that play key roles in protecting plants against fungal attacks (Tran et al., 2022; Salazar et al., 2023; Tuyen et al., 2023). Furthermore, they can protect plants by inducing systemic resistance through the activation of defence and stress signalling pathways (Li et al., 2020; Samaras et al., 2021; Yang et al., 2023), and promote plant growth by phosphate solubilization or the production of phytohormones (Sansinenea, 2019; Blake, Christensen and Kovács, 2021). In addition, bacterial species belonging to the genus *Bacillus* are highly competitive and can tolerate extreme environmental conditions (Ulrich et al., 2018). These features are instrumental in the selection of BCAs and consolidate the numerous studies proposing *Bacillus* spp. as a potential tool to control plant disease (El Hassni et al., 2007a; Dihazi et al., 2012; Slama et al., 2019). Indeed, several studies have investigated the use of *Bacillus* spp. to control the bayoud disease (El Hassni et al., 2007b; Dihazi et al., 2012; Boulahouat et al., 2022), however, there is still a lack of information regarding the characterisation of the genomic features and functional mechanisms underlying the antifungal and PGP properties of the tested *Bacillus* BCAs.

Whole genome sequencing (WGS) has emerged as an indispensable tool in microbial research, offering profound insights into microbial genome architecture and enabling the comprehensive characterization of their taxonomic diversity, functional potential, and ecological roles. When coupled with techniques such as average nucleotide identity (ANI) analysis, WGS facilitates the resolution of closely related species and provides critical insights into their evolutionary adaptations to specific hosts or ecological niches (Liu et al., 2019). Moreover, the annotation of whole genome sequences significantly contributed to the discovery and identification of key *Bacillus* genes that contribute to biocontrol activities such as the production of different secondary metabolites and carbohydrate-active enzymes (CAZymes) involved in fungal cell wall degradation (Li et al., 2022), and genes participating to PGP activities such as siderophore or indole-3-acetic acid (IAA) production (Thomloudi et al., 2021; Wang et al., 2024). For instance, the analysis of several *Bacillus* genomes showed their capacity to encode different secondary metabolites with antifungal activities such as lanthipeptides, fengycin, bacillibactin, bacillaene, or macrolactin H (Feng et al., 2022; Yang et al., 2023). Other studies also showed that different biocontrol bacteria belonging to the *Bacillus* genus harbor genes involved in chitinase, glucanase, and chitin deacetylases secretion, which limit fungal development throughout the breakdown of their cell wall structure (Khan et al., 2018; Li et al., 2025). Extensively, several studies explored PGP genes associated with biocontrol *Bacillus*. For instance, Wang et al. (2024), showed that *B. halotolerans* Q2H2, protecting potato plants against *Fusarium* wilt disease, could efficiently express several PGP traits such as IAA and siderophore production, free nitrogen fixation and phosphate solubilization. The genome analysis of Q2H2 identified a repository of different genes implicated in the expression of identified PGP traits.

The purpose of this study is to explore the biocontrol potential and PGP traits of *B. halotolerans* KFD, isolated from the rhizoplane of date palm, alongside the identification of candidate genes associated with these traits. This work constitutes a step forward in the identification of potential BCAs from the oasis environment against the bayoud disease.

2. Material and methods

2.1. Sampling, bacterial isolation and culture conditions

The sampling was conducted in the oasis of Figuig, Morocco (32°6′36″N, 1°12′53″ W) in February 2023 (Fig. 1). The date palm roots of healthy and infected plants were collected at a depth of 30 cm and stored at 4 °C during transportation to the laboratory. The bacterial isolation was performed by shaking roots for 1 h at 150 rpm in a 250 ml Erlenmeyer containing 100 ml of sterile Phosphate Buffer Saline (PBS, 8 g NaCl; 0.2 g KCl; 1.44g Na_2HPO_4 and 0.245g KH_2PO_4 /L). Serial dilutions were performed on the bacterial suspensions in PBS, plated on Nutrient Agar (NA), and incubated at 30 °C. Based on morphological differences, colonies were picked and sub-cultured in new NA plates. We isolated 40 colonies that were used in downstream analysis. All strains were maintained in 20 % glycerol at −20 °C until use.

2.2. Fungal culture conditions

All fungi used in this study were cultivated on potato dextrose agar (PDA) with an incubation at 28 °C. *Fusarium solani* and *F. oxysporym* f.sp. *lycopersici*, were provided by the Unit of Microbial Biotechnology, Agrosciences and Environment of Cadi Ayyad University, Marrakech. *Botrytis cinerea* and *Phytophtora infestans* were provided by the Phytopathology Unit of the National School of Agriculture in Meknes.

2.3. Selection of KFD isolate, dual plate assays, and antifungal spectrum

The isolated colonies (40 colonies) were pre-screened against Foa on PDA plates to select isolates that had antifungal activities. A fungal plug was cut from an actively growing Foa plate and placed in the middle of a PDA plate. On each plate, two different bacterial isolates were streaked at 2.5 cm from the center of the petri dish on the two opposing sides of the fungal plug. The assay was performed in triplicates and all assay and control plates were incubated at 28 °C for 7 days. Isolates that showed interesting antifungal properties were retrieved from the assay and cultivated on new NA plates. The KFD isolate, obtained from infected roots, was selected for further characterization due to its high antagonistic activity exhibited against Foa. The antifungal activity of KFD against Foa was further confirmed with dual-plate confrontation (Zhu et al., 2020) and we tested its antifungal spectrum against other fungal pathogens, such as *F. oxysporym* f.sp. *lycopersici, F. solani, F. proliferatum, B. cinerea,* and *P. infestans.* The dual-plate confrontation was conducted by culturing the isolate overnight in Tryptic Soy Broth (TSB) media at 30 °C in a shaking incubator. The fungal plug of each pathogen was placed in the center of the petri plate and 10 μL of the bacterial culture was spot-inoculated on opposing sides at 2.5 cm distance from the center of the plate. The control plates were inoculated with 10 μl of sterile TSB. The dual assay was performed in triplicates and incubated at 28 °C. The

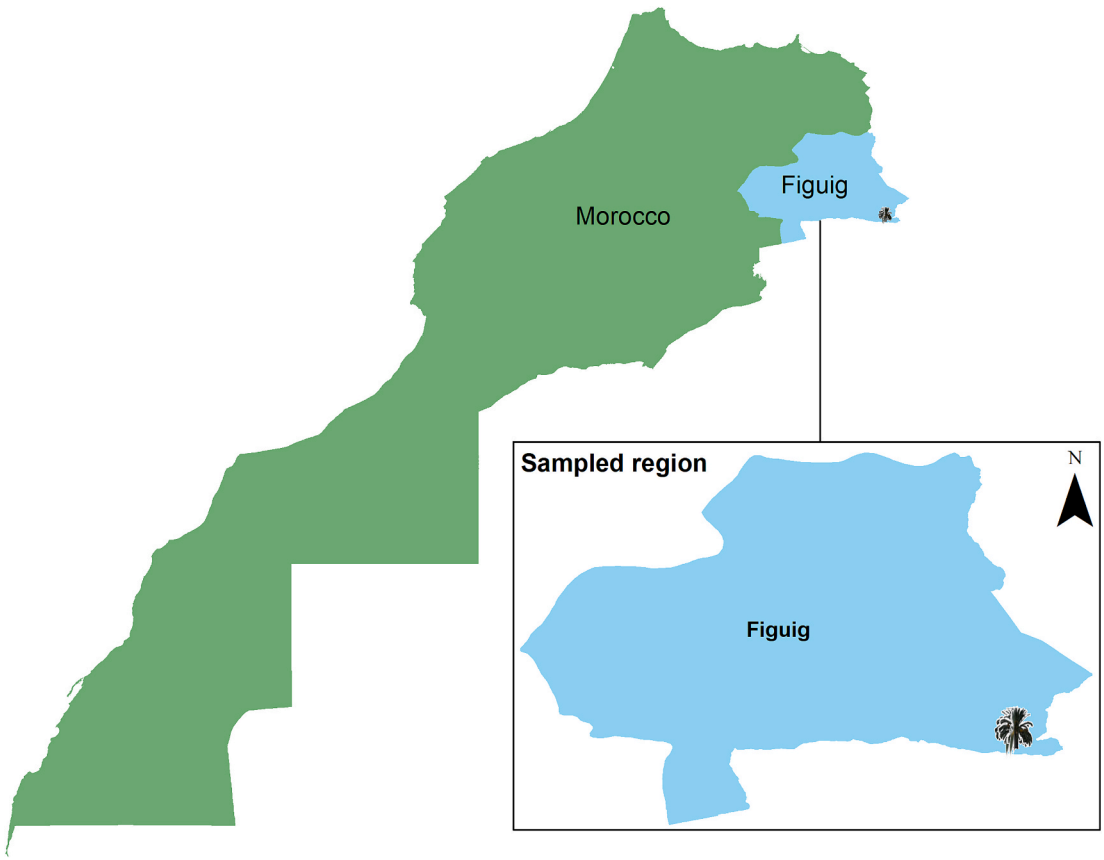

Fig. 1. Moroccan map showing the region of Figuig where the samples were collected. The date palm trees represent the area of the oasis where samples were collected.

percentage inhibition was calculated according to the following formula:

$$PercentageofInhibition = \frac{(C - T)}{C} \times 100$$

C = Control diameter, T = Diameter in co-culture

2.4. Determination of PGP and chitinase activities of B. halotolerans KFD

2.4.1. Inorganic phosphate solubilization

The ability of the isolate to solubilize phosphate was conducted on liquid National Botanical Research Institute's Phosphate (NBRIP) medium (Glucose 10 g, $MgCl_2 \cdot .6H_2O$ 5.0 g, $MgSO_4 \cdot .7H_2O$ 0.25 g, $(NH_4)_2SO_4$ 0.1 g, KCl 0.2 g and $Ca_3(PO_4)_2$ 5.0 g as insoluble phosphate). The assay was performed in triplicate containing 20 ml of NBRIP inoculated with 1 ml of the bacterial culture grown overnight and incubated at 30 °C on a rotary shaker (150 rpm) for seven days. Following incubation, the liquid cultures were centrifuged at 10 000 × g for 10 min and the supernatants were used to assess the phosphate released into the solution using the molybdenum blue colorimetric method.

2.4.2. IAA production

The ability of our isolate to produce IAA was evaluated on Yeast Extract Mannitol broth (Yeast extract 1,0 g, Mannitol 10,0 g, KH_2PO_4 0.5 g, $MgSO_4 \cdot .7H_2O$ 0.2 g, NaCl 0.1 g) with 5 mg/ml of L-tryptophan. One ml of the overnight culture was added to the medium and cultured in triplicate on a rotary shaker (150 rpm) at 30 °C for 5 days and centrifuged at 4,000 rpm for 30 min to collect the supernatant. The IAA production was revealed by mixing 2 ml of the supernatant culture with 4 ml of Salkowski reagent (1 ml of 0.5 M $FeCl_3$ in 49 ml of 35 % (w/v) $HClO_4$). Optical density was read at 530 nm using a spectrophotometer (JANWAY-6405), and the IAA concentration was determined using a pure IAA standard graph.

2.4.3. Siderophore production

The production of siderophores was characterized by using the chrome azurol (CAS) plates technic (Schwyn and Neilands, 1987). The bacteria grown overnight were inoculated on the CAS plate and incubated for 5 days at 30 °C. The assay was performed in triplicate, and the production of orange color around the colonies was considered positive for siderophore production.

2.4.4. Acc-deaminase production

To assess ACC-deaminase production, the bacteria were grown overnight in 5 ml TSB, and the cells were collected by centrifugation at 6000 × g for 10 min. Then, the cells were washed twice with sterile 0.1 M Tris–HCl (pH 7.5) and resuspended in 1 ml of 0.1 M Tris–HCl (pH 7.5). The bacteria were spot inoculated three times on minimal Dworkin and Foster (DF) salt media (4.0 g KH_2PO_4, 6.0 g Na_2HPO_4, 0.2 g $MgSO_4.7H_2O$, 2.0 g glucose, 2.0 g gluconic acid and 2.0 g citric acid with trace elements: 1 mg $FeSO_4 \cdot .7H2O$, 10 mg H_3BO_3, 11.19 mg $MnSO_4 \cdot H_2O$, 124.6 mg $ZnSO_4 \cdot .7H_2O$, 78.22 mg $CuSO_4 \cdot .5H_2O$, and 10 mg MoO_3, pH was adjusted to 7.2). The DF media was amended with 3 mM ACC instead of $(NH_4)_2SO_4$ as the sole nitrogen source (Dworkin and Foster, 1958). The assay was performed in triplicate, and the inoculated plates were incubated at 30 °C for 3 days. Colonies growing on the plates are considered ACC deaminase producers.

2.4.5. Nitrogen fixation

The ability of the isolate to fix free nitrogen was assessed on Norris glucose nitrogen free media (Glucose 10.0 g, Dipotassium phosphate 1.0 g, Magnesium sulphate 0.2 g, Calcium carbonate 1.0 g, Sodium chloride

0.2 g, Sodium molybdate 0.005 g, Ferrous sulphate 0.1 g pH 7.0 ± 0.2) supplemented with l ml of the overnight culture and kept at 30 °C for 2 days to observe the growth. The assay was performed in triplicate and the observation of bacterial growth after incubation indicated free nitrogen fixation.

2.4.6. Chitinase assay

The chitinase activity was conducted to verify the ability of our isolate to degrade chitin, which is an important component of fungal cell walls. The extraction of colloidal chitin was completed as described by Koteshwara (2021). The colloidal chitin agar (CCA) was prepared as described by Saima et al. (2013) and the test was conducted by spotting tree spots of the overnight culture on the CCA. The assay was conducted in triplicate and incubated at 30 °C for 5 days.

2.5. Greenhouse evaluation of the biocontrol efficacy of B. halotolerans KFD on date palm seedlings

Greenhouse pot experiments were performed to evaluate the biocontrol efficacy *B. halotolerans* KFD on Foa. The experiment was carried out on 3-month-old date palm plants in pots containing soil, peat, and sand 2:2:1 (v/v/v). KFD were cultivated on NA plates and incubated at 30 °C for 24H. After incubation, a colony was picked and inoculated in Luria-broth medium. The inoculated broth was incubated at 30 °C on a shaking incubator (150 rpm) for 48 h. The culture was centrifuged at 6000xg for 15 min and re-suspended in PBS to a final concentration of 1×10^8 CFU/mL. To collect the fungal pathogen spores, Foa was cultured on PDA and incubated at 28°c for 10 days. Sterile ultrapure water was poured on the plates, and the conidia were collected by scratching the agar. The spore suspension was filtered with four layers of gauze to remove fungal hyphae. The filtered spore solution was adjusted to a final concentration of 1×10^6 spores/mL using a hemocytometer. The roots of date palms seedlings were first immersed in KFD cell suspension before being treated with Foa. The control was treated with water. The experiment consisted of four different treatments: (T1) plants treated with water only, (T2) plants inoculated with KFD only, (T3) plant inoculated with KFD and Foa, (T4) plants treated with Foa only. Each treatment consisted of five seedlings. After five months, the disease incidence rate was measured based on the following formula: $.Disease\ incidence\ rate = \frac{number\ of\ diseased\ plants}{number\ of\ tested\ plants} \times 100$

2.6. DNA extraction, genome sequencing, data processing and functional annotation

The DNA extraction was conducted with the isolate grown overnight on TSB at 30 °C in a shaking incubator. Using the commercial QIAamp DNA Mini Kit (Qiagen, Germany) following the manufacturer's instructions. Genomic DNA was sheared randomly into short fragments. The fragments obtained were end-repaired, A-tailed, and ligated using Illumina adapters. Following size selection, fragments were amplified and purified. The library was quantified using Qubit and quantitative PCR, and size distribution was detected using an Agilent 5400 fragment analyzer. The quantified libraries were pooled and sequenced on the Illumina NovaSeq6000 platform as 2x250. The quality of the reads was evaluated with FastQC v.02. Reads were assembled using spades (Prjibelski et al., 2020), and the assembled genome was annotated using Prokka (Seemann, 2014). The predicted genes were further annotated with the NCBI non-redundant (NR), UniProtKB/Swiss-Prot, CAZY, COG, and KEGG databases. The secondary metabolite gene clusters were predicted using antiSMASH (https://antismash.secondarymetabolites.org/). Secreted proteins were predicted using SignalP (Almagro Armenteros et al., 2019). The circular format of the genome was obtained with Circos.

2.7. Phylogenomics and comparative genomics analysis

The twenty genomes that showed the highest similarity with our isolate, after BLAST against the NCBI database, were retrieved for phylogenomic analysis. The clustering of the different gene families was computed using Orthofinder (Emms and Kelly, 2019), the evolutionary distance was calculated using the maximum likelihood tree inference method with 500 bootstrap replicates using Mega software (https://www.megasoftware.net), and the tree was visualized with ITOL (https://itol.embl.de). Average Nucleotide Identity (ANI) analysis was performed with Pyani (https://huttonics.github.io/pyani/) using the ANIm method, and the digital DNA-DNA hybridization (dDDH) was computed using the genome-to-genome distance calculator online tool from ggdc.dsmz.de/ggdc.php#. The analysis of core, unique and accessory genes was done using the cd-hit cluster program (Fu et al., 2012).

2.8. Statistical analysis

Statistical analysis were conducted using IBM SPSS software with one-way analysis of variance (ANOVA). Significant differences between the means were evaluated using Tukey's multiple comparison test at a P value cutoff <0.05. Statistical analyses of the genome were computed using QUAST (Gurevich et al., 2013) and the completeness of the genome was evaluated with BUSCO (Manni et al., 2021).

3. Results

3.1. Evaluation of the in vitro antifungal activity, PGP traits, chitinase activity, and in vivo biocontrol efficacy of B. halotolerans KFD

The antifungal activity ability of *B. halotolerans* KFD was evaluated by dual confrontation plate assays against the bayoud's pathogen Foa and several other plant fungal pathogens, namely *F. oxysporym* f.sp. *lycopersici, F. solani, F. proliferatum, B. cinerea,* and *P. infestans,* to verify the spectrum of its antimicrobial activity. The results showed that *B. halotolerans* KFD could effectively inhibit the growth of all tested phytopathogens with percentages of inhibition between 69.41 % and 78.03 % (Table 1, Fig. 2A, and Table S1). To verify the ability of KFD to promote plant growth, we analysed some PGP traits. The obtained results showed that *B. halotolerans* KFD has the capacity to solubilise phosphate (26.96 mg/L), produce IAA (5,73 µg/ml), siderophores, ACC deaminase, and fix free nitrogen. Furthermore, KFD demonstrated the ability to grow on a medium containing chitin as the only carbon source, suggesting its potential to produce chitinase, despite the absence of a clear hydrolysis zone around the colony (Table 2 and Fig. S1). Beyond the *in vitro* inhibition test, *B. halotolerans* KFD was tested against Foa under greenhouse conditions. We observed that after five months of co-cultivation, *B. halotolerans* KFD significantly reduced the disease symptom index (DSI) on date palm seedlings compared to untreated controls (Fig. 2B).

3.2. Assembly and annotation of B. halotolerans KFD

To investigate the functional characteristics of *B. halotolerans* KFD, we performed WGS. KFD has a genome size of 3,952,925 bp with a GC content of 43,89 % (Fig. 3). The N50 value of the assembled genome is 1,047,934 bp, and the assessment of completeness with Busco showed that all the bacterial genes were present. The prediction of the coding sequences (CDS) reported 3,902 CDSs with 78 tRNA, four rRNA, and one tmRNA. Of the 3,902 CDS, 3,893 had similarities with the NCBI NR database, and 3,735 showed similarities with the UniProtKB/Swiss-Prot database. The COG database classified 3,103 sequences into COG functional categories, accounting for 79,52 % of the total sequences, while 2,373 genes were annotated with KEGG database. KEGG and COG annotations reported the presence of substantial microbial functions

Table 1
Percentages of inhibition of the *in vitro* screening of *B. halotolerans* KFD against tested phytopathogens.

Pathogen	*F. proliferatum*	Foa	*F. solani*	*P. infestans*	*B. cinerea*	*F. oxysporym* f.sp. *lycopersici*
Inhibition (%)	78.03± 0.67a	76.86± 0.67ab	75.29± 0.00abc	74.50± 2.44bc	72.94± 0.00c	69.41± 1.17d

Data are means ± SD. The lowercase letters indicate significant differences ($p < 0.05$).

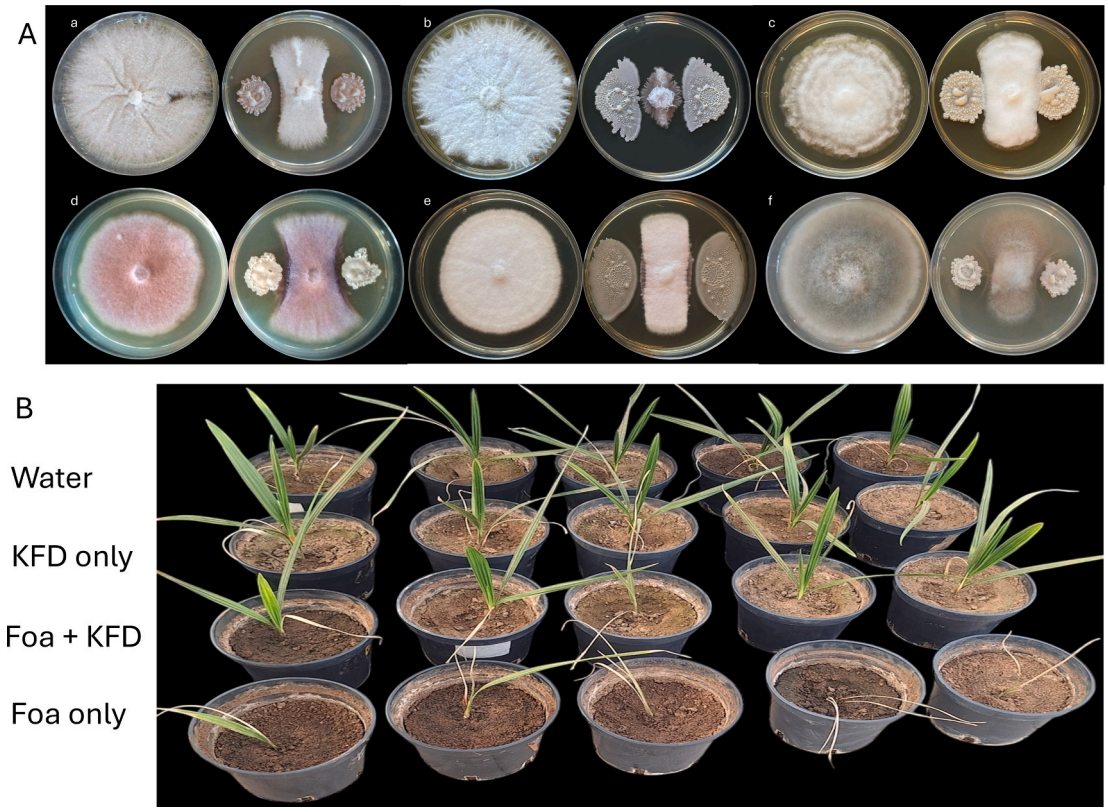

Fig. 2. Dual-plate confrontation and greenhouse assay of *B. halotolerans* KFD against Foa. (A) inhibition assay of (a) Foa, (b) *F. proliferatum*, (c) *P. infestans*, (d) *F. solani*, (e) F. oxysporym f.sp. *lycopersici* and (f) *B. cinerea* by *B. halotolerans* KFD. (B) Greenhouse assay showing date palm seedlings with different treatments and the disease incidence rates.

Table 2
Characterization of PGP traits and chitinase activity of *B. halotolerans* KFD.

P solubilization	Siderophore production	IAA production	Nitrogen fixation	ACC deaminase	Chitinase activity
+	+	+	+	+	+

implicated in antagonistic and PGP activities. These functions were related to the biosynthesis and transport of secondary metabolites, environmental information processing, cell motility, and inorganic ion transport and metabolism as represented on Fig. 4.

3.3. Analysis of biosynthetic gene clusters to predict secondary metabolites production

The profiling of biosynthetic gene clusters (BGC) in the genome of *B. halotolerans* KFD revealed the presence of 11 gene clusters (Table S2), with three non-ribosomal peptide synthetases (NRPS), one sactipeptide, two terpenes, one T3PKS, one unspecified type, and three hybrids. Bacillibactin, bacilysin, and bacillaene showed 100 % similarity with known BGCs clusters in the database. Cluster 2 showed 87 % similarity with subtilosin A, cluster 6 showed 80 % similarity with fengycin, cluster 8 showed 5 % similarity with laterocidine, cluster 9 showed 39 % similarity with surfactin and cluster 10 showed 15 % similarity with plipastatin. The genes coding these clusters are listed in Table 3.

3.4. Analysis of carbohydrate active enzymes and enzymes involved in fungal cell wall degradation

The annotated amino acid sequences of *B. halotolerans* KFD were aligned with the CAZY database to predict genes encoding CAZymes. The annotation (Fig. 5) showed that *B. halotolerans* KFD harbors 110 Glycoside Hydrolases (GHs), 70 Glycosyl Transferases (GTs), 56 carbohydrate-binding modules (CBMs), 17 Carbohydrate Esterases (CEs), 11 Polysaccharide Lyases (PLs), and one enzyme involved in auxiliary Activities (AAs). The GH family was divided into 33 subfamilies. The main subfamilies were GH1, GH4, GH13, GH131 GH18, and GH32. The GTs, divided into 12 subfamilies, were dominated by GT2 and GT4. The CBMs family contained 11 subfamilies, and the major subgroup was CBM5O. The CEs group was divided into 6 subfamilies dominated by CE4 and CE12. The presence of chitinase enzymes such as

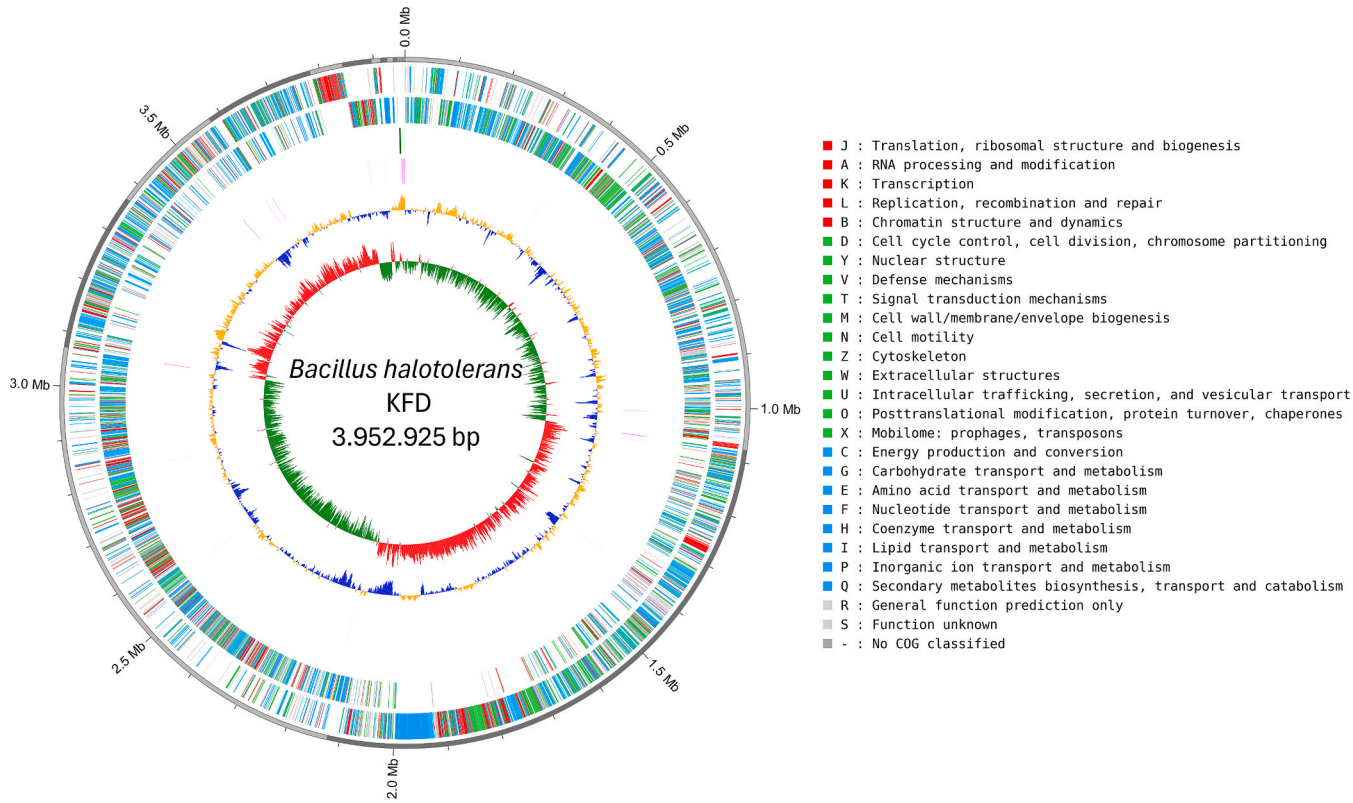

Fig. 3. Genome visualization of *B. halotolerans* KFD: the outermost circle represents the size of the genome, the second and third circles represent the forward and reverse strand, the fourth circle represents rRNAs, and the fifth represents tRNAs. The two innermost circle represent the GC content and GC skew, respectively.

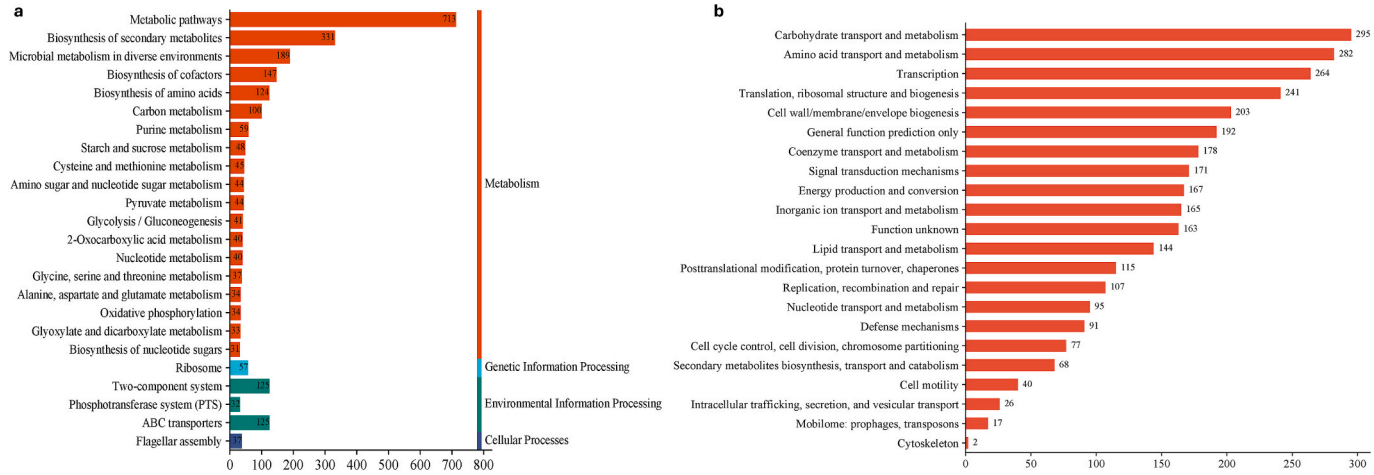

Fig. 4. Functional annotation of *B. halotolerans* KFD: (a) KEGG pathway analysis and distribution of genes across the different pathways (b) gene classification into COG categories.

GH18 and GH23 can significantly contribute to the antifungal activity of KFD.

3.5. Analysis of genes linked to plant growth-promotion

The PGP traits of *B. halotolerans* KFD for phosphate solubilization, IAA, ACC deaminase and siderophore production were confirmed *in vitro*. Therefore, we conducted a genome mining study to identify the key genes involved in PGP characteristics. For the metabolism and transport of inorganic phosphate (P_i), we identified 10 genes: *pstA, pstB, pstC, pstS, ykaB, ykaA, cysP, yjkB, yqgI, yqgH, phoP,* and *phoR*. These genes mainly encode transmembrane proteins that are crucial for the transport of P_i across cell membranes, except for the *phoP* and *phoR* genes that intervene in the regulation of P_i under excess and deficiency conditions. Furthermore, the *pstABCS* genes encoding phosphate transporters were also detected in the phosphate metabolic pathway (Fig. S2). We also annotated in *B. halotolerans* KFD genes linked to tryptophan biosynthesis, a precursor to IAA, which is a key plant hormone involved in various growth processes such as cell elongation, root initiation, and fruit development. T*rpABCDEFP* genes, responsible for the production and transport of tryptophan, were detected in the genome. Furthermore, we identified the enzyme aldehyde dehydrogenase, which is implicated in IAA production using tryptophan as a precursor. The KEEG pathway analysis also identified the pathway for

Table 3
Genes involved in antibiotic biosynthesis in the *B. halotolerans* KFD genome.

Protein name	Gene Name	Biological process	Protein name	Gene Name	Biological process
3-oxo-glucose-6-phosphate: glutamate aminotransferase	*ntdA*	antibiotic biosynthetic process	Polyketide biosynthesis acyl-carrier-protein	*acpK*	antibiotic biosynthetic process
Fengycin synthase-activating enzyme	*sfp*	antibiotic biosynthetic process	Polyketide biosynthesis acyltransferase homolog	*pksD*	antibiotic biosynthetic process
Bacilysin biosynthesis	*bacC*	antibiotic biosynthetic process	Polyketide biosynthesis malonyl CoA-acyl carrier protein transacylase	*pksC*	antibiotic biosynthetic process
Bacilysin biosynthesis	*bacG*	antibiotic biosynthetic process	Polyketide biosynthesis malonyl-ACP decarboxylase	*pksF*	antibiotic biosynthetic process
Bacilysin biosynthesis	*bacA*	antibiotic biosynthetic process	Polyketide biosynthesis PsE	*pksE*	antibiotic biosynthetic process
Bacilysin biosynthesis	*bacB*	antibiotic biosynthetic process	Polyketide synthase	*pksJ*	antibiotic biosynthetic process
Bacilysin synthetase	*bacD*	antibiotic biosynthetic process	Polyketide synthase	*pksL*	antibiotic biosynthetic process
Bacilysocin biosynthesis protein	*ytpA*	antibiotic biosynthetic process	Polyketide synthase	*pksM*	antibiotic biosynthetic process
Beta-lactamase	*bla*	beta-lactam antibiotic catabolic process	Probable beta-lactamase	*ybxI*	antibiotic catabolic process
Kanosamine-6-phosphate phosphatase	*ntdB*	antibiotic biosynthetic process	Probable polyketide biosynthesis enoyl-CoA hydratase	*pksH*	antibiotic biosynthetic process
Linear gramicidin synthase subunit B	*lgrB*	antibiotic biosynthetic process	Probable polyketide biosynthesis zinc-dependent hydrolase	*pksB*	antibiotic biosynthetic process
Plipastatin synthase subunit A	*ppsA*	amino acid activation for nonribosomal peptide biosynthetic process	Putative polyketide biosynthesis enoyl-CoA isomerase	*pksI*	antibiotic biosynthetic process
Plipastatin synthase subunit B	*ppsB*	amino acid activation for nonribosomal peptide biosynthetic process	Surfactin synthase subunit 1	*srfAA*	amide biosynthetic process, antibiotic biosynthetic process
Plipastatin synthase subunit C	*ppsC*	amino acid activation for nonribosomal peptide biosynthetic process	Surfactin synthase subunit 2	*srfAB*	amino acid activation for nonribosomal peptide biosynthetic process
Plipastatin synthase subunit D	*ppsD*	antibiotic biosynthetic process	Surfactin synthase subunit 3	*srfAC*	amino acid activation for nonribosomal peptide biosynthetic process
Plipastatin synthase subunit E	*ppsE*	amino acid activation for nonribosomal peptide biosynthetic process	Surfactin synthase thioesterase subunit	*srfAD*	antibiotic biosynthetic process
Polyketide biosynthesis	*pksS*	antibiotic biosynthetic process	Transaminase	*bacF*	antibiotic biosynthetic process
Polyketide biosynthesis	*pksG*	acetyl-CoA metabolic process, antibiotic biosynthetic process	Virginiamycin B lyase	*vgb*	antibiotic catabolic process

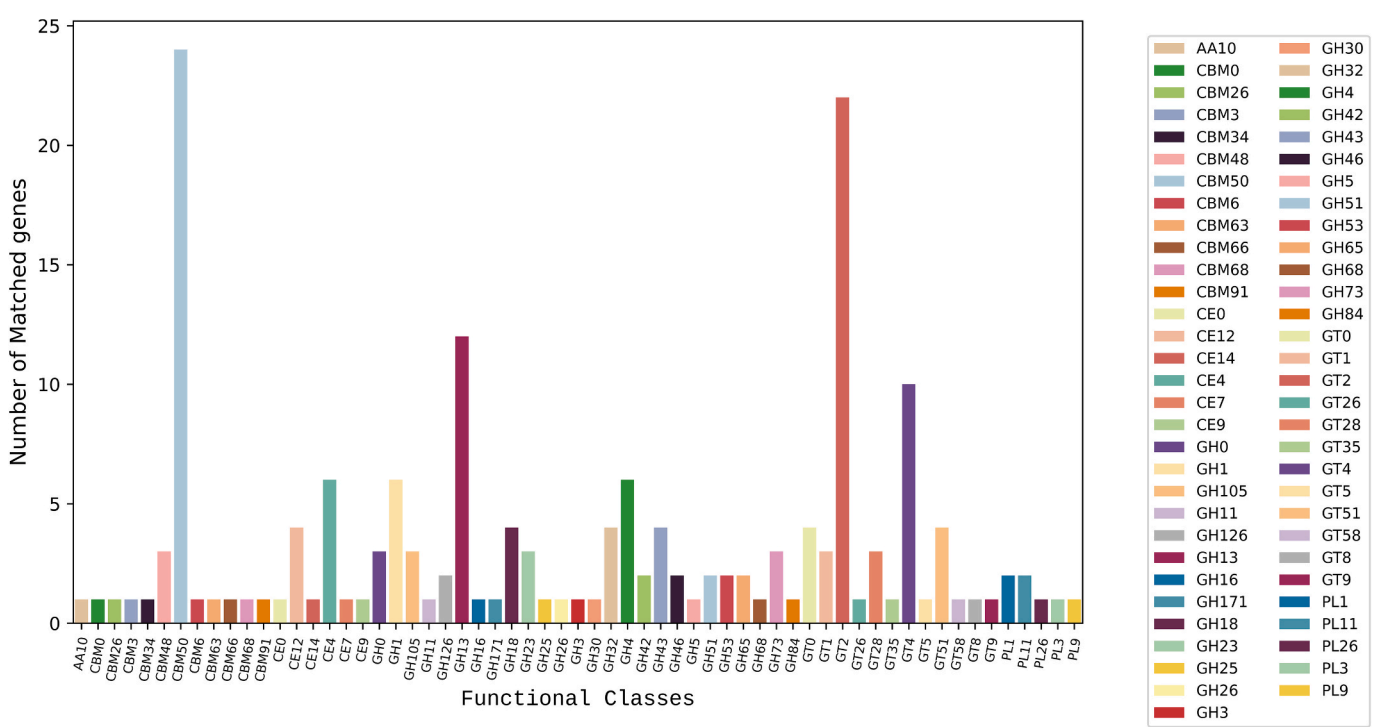

Fig. 5. Carbohydrate active enzymes class and subclass prediction: Glycoside Hydrolases (GHs), Glycosyl Transferases (GTs), Polysaccharide Lyases (PLs), Carbohydrate Esterases (CEs), Auxiliary Activities (AAs), Carbohydrate-binding modules (CBMs).

tryptophan metabolism and biosynthesis as well as the siderophore biosynthesis pathway (Fig. S3–S5). Concerning the siderophore production and iron transport into the cell, we annotated 12 genes implicated in this process. We also detected the *yutI* gene implicated in the fixation of nitrogen (Table 4).

3.6. Prediction and annotation of B. halotolerans KFD secreted proteins

Bacterial cellular machinery secretes different products to interact with plants. These proteins and peptides must be transported outside the microbial cell, throughout the bacterial cell membrane and wall, thanks to signal peptides. Therefore, we attempted to predict the signal peptides secreted by *B. halotolerans* KFD using the SignalP program. We predicted 135 lipoprotein signal peptides (Lipo), 265 standard signal peptides (SP), and 6 twin-arginine translocation (TAT) signal peptides. Moreover, we retrieved and annotated the sequences predicted to be secreted. Among the annotated genes, we detected genes involved in antifungal compound production, namely subtilisin E, plipastatin, bacillolysin, *N*-Acetylglucosaminidase, and β-glucanase (Table S3). We also detected in the secreted proteins the GlcNAc-binding protein A intervening in the attachment to chitin. These secreted antifungal molecules probably underlie the antagonistic activity of *B. halotolerans* KFD against the reported fungal pathogens.

3.7. Comparative genomics analysis and investigation of genes specific to B. halotolerans KFD

We blasted different sequences of the KFD genome against the NCBI database and found that it is a *B. halotolerans* species. The sequences of the most similar species were downloaded for species comparative analysis. First, orthologous gene analysis was performed, and the phylogenomic tree was drawn based on the orthogroups (Fig. 6). Taxonomy analysis showed that *B. halotolerans* KFD's closest strains were *B. halotolerans* strain ZB201702, *B. halotolerans* strain KKD1, *B. halotolerans* strain F41-3, *B. halotolerans* strain Q2H2, and *B. halotolerans* strain LN2. We further analyzed the ANI between KFD and its closest relatives (Table 5 and Fig. S6). The ANI comparison of our genome confirmed the results from the NCBI database that our isolate was a member of *B. halotolerans*.

We compared the BGCs secreted by the six closest organisms using antiSMASH. Except for the plipastatine-encoding BGC, all other BGCs were shared among the six strains with several variations in the degree of similarity (Table 6). The BGCs bacillibactin, bacillaene, and bacilysin shared a 100 % similarity across all the strains. The subtilisin A cluster was also similar across all the organisms but shared less similarity with *B. halotolerans* KFD. The surfactin-encoding clusters of the compared strains showed 86 % similarity with known clusters, however, they shared less similarity with the surfactin-encoding cluster of *B. halotolerans* KFD, with 39 % similarity. For the fengycin encoding cluster, we observed similarities between strain KFD and strain ZB201702, which shared 80 % similarity with known clusters, compared to the other strains, which shared 100 % similarity. The laterocidine cluster showed only 5 % similarity with the known clusters, and this was observed across all strains. The plipastatine-encoding cluster was missing in four strains but was present in ZB201702 and KFD, at 53 % and 15 %, respectively. These results further confirm the similarity between KFD and ZB201702 as reported in the ANI analysis.

After comparing the BGCs, we investigated the gene similarities and dissimilarities between the six strains, clustered the homologous genes, and extracted the core accessory and unique genes from each genome. The pangenome analysis reported a total of 3750 core genes shared among all six strains and 630 accessory genes (Fig. 7). Furthermore, we identified 146 unique genes in the genome of *B. halotolerans* KFD. The annotation of these unique genes revealed that several encoded toxins located between the plasma membrane and the extracellular region (Table S4). Furthermore, we detected the plipastatin synthase subunit D gene, which belongs to the plipastatine cluster. This cluster wasreported earlier in the BGCs comparative analysis and were missing in four of the compared strains and showed high variations between KFD and ZB201702.

4. Discussion

Menaces caused by the fungal pathogen Foa have long been a serious concern and have attracted considerable attention to the development of management strategies (Benzohra et al., 2015; Abouamama et al., 2018). Resorting to BCAs is a promising management strategy and eco-friendly alternative that can reduce chemical fingerprints (Collinge et al., 2022; Haq et al., 2024). In this work, we report the antifungal and biocontrol properties of a new strain of *B. halotolerans* that showed

Table 4
Genes associated with PGP Traits in the *B. halotolerans* KFD genome.

PGP trait	Gene name	Function	PGP trait	Gene name	Function	PGP trait	Gene name	Function
Siderophore production	*ybdZ*	Siderophore biosynthetic process	**Phosphate solubilization**	*ykaB*	Phosphate ion transport	**IAA**	*trpP*	Tryptophan transporter
	dhbE	Siderophore biosynthetic process		*ykaA*	Phosphate ion transport		*trpS*	Tryptophanyl-tRNA synthetase
	yvrB	siderophore-dependent iron import into cell		*cysP*	Phosphate ion transport		*rtpA*	Tryptophan RNA-binding attenuator protein inhibitory protein
	fhuG	siderophore-dependent iron import into cell		*yjkB*	Phosphate ion transport		*trpA*	Tryptophan biosynthetic process
	fhuB	siderophore-dependent iron import into cell		*yqgI*	Phosphate ion transport		*trpB*	Tryptophan biosynthetic process
	yfmE	siderophore-dependent iron import into cell		*yqgH*	Phosphate ion transport		*trpC*	Tryptophan biosynthetic process
	yfmD	siderophore-dependent iron import into cell		*pstB*	Phosphate ion transport		*trpF*	Tryptophan biosynthetic process
	yfiZ	siderophore-dependent iron import into cell		*pstA*	Phosphate ion transport		*trpD*	Tryptophan biosynthetic process
	yfhA	siderophore-dependent iron import into cell		*pstC*	Phosphate ion transport		*trpE*	Tryptophan biosynthetic process
	yclN	siderophore-dependent iron import into cell		*pstS*	Phosphate ion transport		*trpG*	Tryptophan biosynthetic process
	yclO	siderophore-dependent iron import into cell		*phoR*	Phosphate transport regulator	**Nitrogen Fixation**	*yutI*	Nitrogen fixation

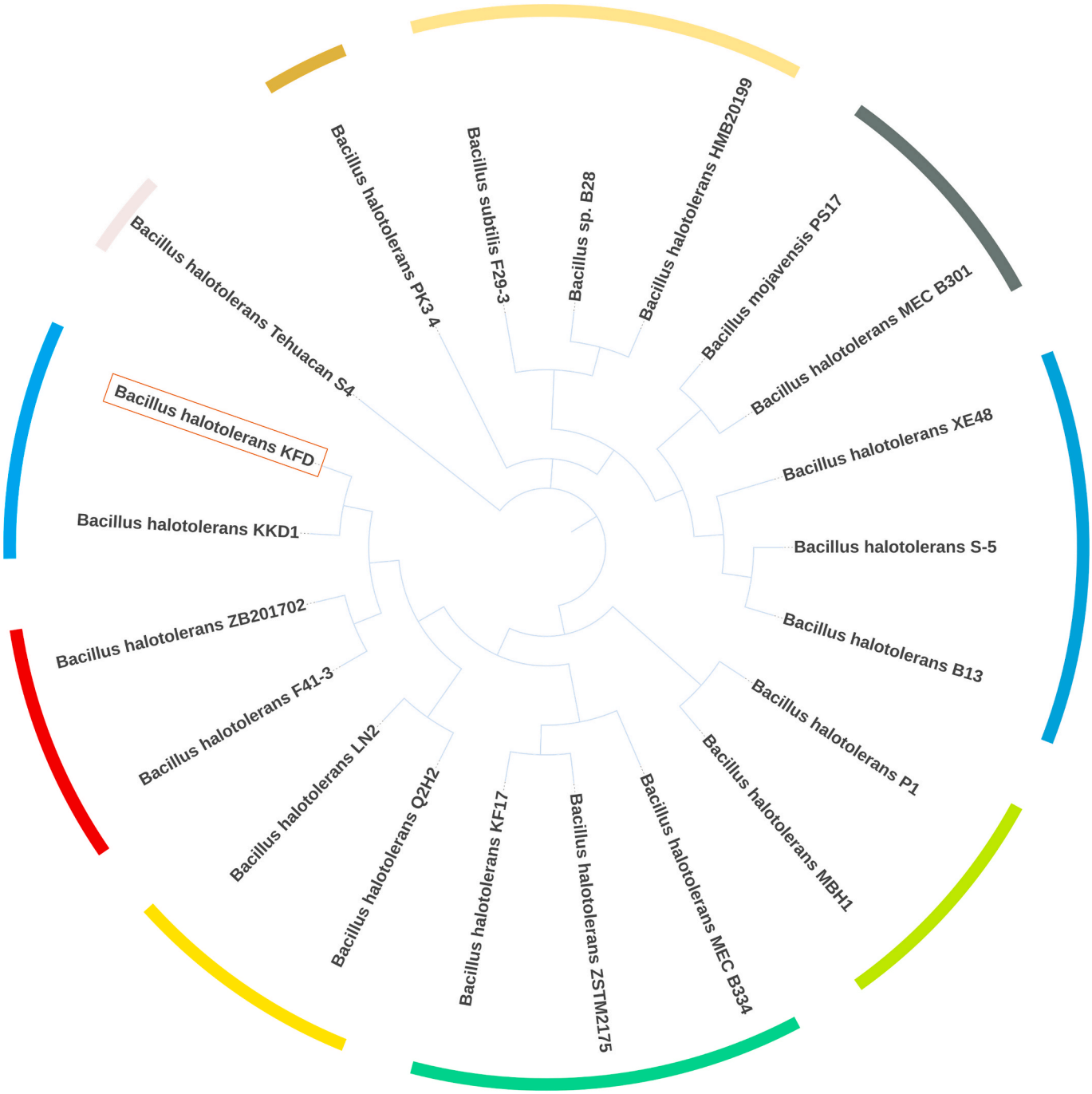

Fig. 6. Phylogenomic tree showing the evolutionary relationship between *B. halotolerans* KFD and 20 closest strains.

Table 5
ANI and dDDH comparison between *B. halotolerans* KFD and closely related strains.

Compared organism	ANI value	dDDH value
Bacillus halotolerans strain ZB201702	0.980375414184475	82.5
Bacillus halotolerans strain KKD1	0.980230413170285	82
Bacillus halotolerans strain F41-3	0.980162070291965	82.3
Bacillus halotolerans strain Q2H2	0.980134273477527	82.4
Bacillus halotolerans strain LN2	0.979838260727567	81.8

interesting features in promoting plant growth as well. Furthermore, we conducted a whole genome analysis to identify (i) the antimicrobial compounds produced by the strain to inhibit fungal pathogens and (ii) the genes linked to PGP activities.

We isolated a root-associated bacterium that was tested using dual-plate methods against the bayoud pathogen Foa, as well as *F. lycopersisi, F. solani, F. proliferatum, B. cinerea, and P. infestans.* KFD was able to hamper the growth of all the tested pathogens, which confirmed that KFD can secrete antifungal molecules. The greenhouse evaluation of the biocontrol efficacy of KFD on date palm seedlings against Foa was consistent with the *in vitro* results. We observed that KFD could effectively limit the occurrence of bayoud disease on date palm and, therefore, represents a potential biocontrol candidate to manage palm dieback disease. Additionally, we established that KFD could secrete different PGP compounds, among which ACC deaminase is important in mitigating plant stress. It was reported that bacteria producing this compound showed a strong protective effect against fungal

Table 6
BGC comparison between *B. halotolerans* KFD and its five closest relatives.

	Bacillibactin	Surfactin	Bacillaene	Fengycin	Laterocidine	Subtilosin A	Bacilysin	Plipastatin
KFD	100 %	39 %	100 %	80 %	5 %	87 %	100 %	15 %
KKD1	100 %	86 %	100 %	100 %	5 %	100 %	100 %	Missing
ZB201702	100 %	86 %	100 %	80 %	5 %	100 %	100 %	53 %
Q2H2	100 %	86 %	100 %	100 %	5 %	100 %	100 %	Missing
LN2	100 %	86 %	100 %	100 %	5 %	100 %	100 %	Missing
F41-3	100 %	86 %	100 %	100 %	5 %	100 %	100 %	Missing

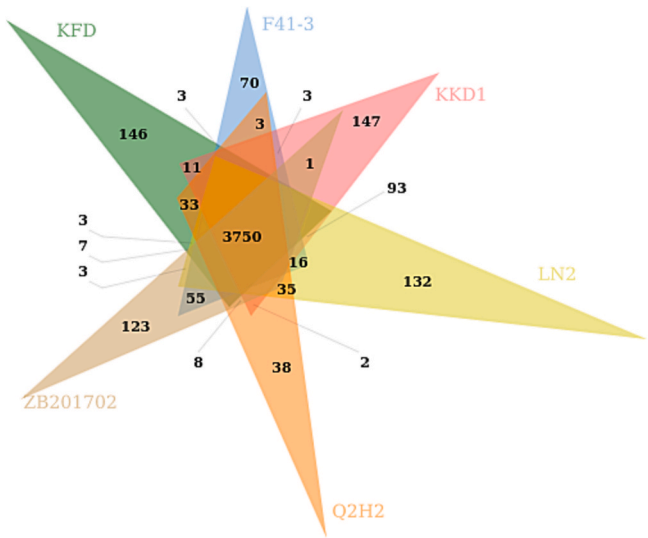

Fig. 7. Pangenome analysis between *B. halotolerans* KFD and the five closest strains showing the core accessory and unique genes.

pathogens such as *Scelerotium rolfsii* (Dixit et al., 2016), *Peronospora* sp. (Barnawal et al., 2017), and *Fusaium* spp. (Donate-Correa et al., 2005). Therefore, the effective secretion of this molecule by *B. halotolerans* KFD can significantly contribute to protecting date palm against Foa.

To identify and investigate the genomic features that harbor the ability of the isolate to produce antifungal compounds and display PGP traits, we performed whole-genome sequencing. The taxonomic assignment of our isolate showed that it belongs to *B. halotolerans* species. To distinguish between the different strains matching our query, we downloaded the 20 most similar strains used for phylogenomic studies. In addition to the phylogenomic analysis, we performed a comparative genomics analysis with the most closely related species. The ANI comparison confirmed that our isolate is a member of *B. halotolerans*. ANI has emerged as a standard tool in comparative genomics and species delineation (Ciufo et al., 2018). It can compute genome similarity comparisons based on the shared orthologous genes of different genomes and discriminate between close relatives depending on a cutoff value of generally 95 %, which indicates, if equal or higher, that the compared genomes belong to the same species. Previous research reported the ability of *B. halotolerans* to inhibit the growth of plant pathogens such as Foa, *F. oxysporum, F. solani, F. acuminatum, F. chlamydosporum, Alternaria alternata, P. infestans,* and *R. bataticola* (Slama et al., 2019), *B. cinerea* (Thomloudi et al., 2021; Wang et al., 2021), *F. pseudograminearum* (Li et al., 2022), *F. oxysporum, F. commune, F. graminearum, F. brachygibbosum, F. oxysporum f. sp. radicis-lycopersici, Rhizoctonia solani, Stemphylium solani* (Feng et al., 2022; Wang et al., 2024), These findings highlight the potential of *B. halotolerans* as potential BCAs in plant diseases management and our study provides evidence of its antagonistic activity against *F. proliferatum,* causing similar symptoms to bayoud disease on date palms (Abdalla et al., 2000). Moreover, our study is the first to describe the isolation of *B. halotolerans* from date palm compartments.

The ability of bacteria to hamper fungal pathogens' development is mainly driven by the secretion of secondary metabolites (Gwa and Ekefan, 2024). We detected from the genomic analysis the presence of 11 BGCs, among which cluster 9 encoding surfractin and cluster 10 encoding plipastatin, based on the percentage similarity with known clusters, could represent new types of corresponding BGCs. Furthermore, cluster 8, which encodes laterocidine with a relatively low similarity to the known clusters (5 %), could be a new secondary metabolite and requires further characterization. The analysis of the BGCs has drawn up a similar profile of the secondary metabolites secreted by KFD compared to other *B. halotolerans* strains, while some secondary metabolites were strain-specific. For instance, the presence of surfractin, bacillaene, fengycin, bacilysin, bacillibactin, and subtilisin A was reported in strains Q2H2, Hil4, Cal.l.30, and LDFZ001 (Slama et al., 2019; Thomloudi et al., 2021; Feng et al., 2022; Tsalgatidou et al., 2022; Wang et al., 2024). However, the presence of kijanimicin was only reported in strain LDFZ001while mycosubtilin was only detected in strain Hil4, and Kalimantacin A only detected in strain Cal.l.30. Seemingly, strain KFD harboured BGCs not reported in the BGCs analysis of the other strains, namely laterocidine and plipastatin. While laterocidine is principally an antibacterial metabolite (Ballantine et al., 2023), plipastatin was reported to show strong antifungal activity against *F. oxysporum* f. sp. *Cucumerinum* (Gao et al., 2017), *F. graminearum,* and *B. cinerea* (Gong et al., 2015; Kiesewalter et al., 2021). The mode of action of plipastatin is not yet characterized, however, it is believed to be involved in the inhibition of fungal phospholipase A_2 and forming pores in their membranes (Harwood et al., 2018). The annotation of secreted proteins detected a signal peptide associated with the plipastatin gene, indicating that this antifungal compound directly interacts with fungal pathogens. Moreover, comparative genomic analysis reported the presence of unique genes in the genome of KFD that are involved in plipastatine biosynthesis. Therefore, we believe that plipastatine could play a role in the biocontrol properties of KFD. However, advanced experiments are required to better determine the role of plipastatine in the antifungal activity of *B. halotolerans* KFD.

Chitin is one of the main components of pathogenic fungi's cell wall. Chitin hydrolysis can be catalyzed by chitinase to produce N-acetylglucosamine, which destroys the structure of the fungal cell wall. The presence of chitinase has been reported to play a substantial role in *B. halotolerans* biocontrol activities against plant fungal pathogens (Slama et al., 2019; Wang et al., 2021, 2024). Through our experiment, we showed that KFD can effectively grow on CCA and therefore can produce chinolytic enzymes. Moreover, CAZymes annotation in the genome of *B. halotolerans* KFD reported the presence of GH18 and GH23 subgroups directly involved in chitinase activities (https://www.cazy.org/Glycoside-Hydrolases.html). GH18 also contains *N*-Acetylglucosaminidase that participates in chitin degradation (Gaderer et al., 2017). The GH30, GH5, and GH26 subfamilies secrete different forms of glucanase that can also degrade glucan in fungal cell walls. We also detected the presence of CBM50, which are modules reported to bind chitin-degrading enzymes such as GH18 and GH23 (https://www.cazy.org/Carbohydrate-Binding-Modules.html). Moreover, we noticed the presence of lytic chitin monooxygenase, AA10, which can destroy the structural organisation of chitin in fungal cell walls (Pan et al., 2023).

Moreover, we were also able to identify different genes related to PGP traits and the detection of these genes, linked to the positive *in vitro* assays, confirms that their effective expression by *B. halotolerans* KFD, placing it as a potential biocontrol microorganism with a protective role against fungal phytopathogens and a positive impact on plant growth and development.

Our findings suggest that *B. halotolerans* KFD could show promising applications in agriculture due to its wide-spectrum antifungal activity that could suppress different plant pathogens, but also thanks to its ability to produce PGP compounds. One of the main concerns about the effective use of microbial BCAs is their environmental adaptability (Yi, et al., 2025). The effectiveness of biocontrol is notably affected by environmental conditions. *B. halotolerans* KFD, isolated from oases, characterized by an extreme environment, represents one of the most adapted candidates to manage the bayoud pathogen prevalent in the same environment. According to the literature, only Slama et al., 2019 reported the use of *B. halotolerans* as a potential candidate against the bayoud disease. However, the *B. halotolerans* they reported, which showed effective *in vitro* results, was isolated from the roots of *Limoniastrum monopetalum* and the rhizosphere of wheat plant. The survival of these bacteria in the oasis environment can be quite questionable. Moreover, the ability to colonize date palm roots could be challenging. In contrast, *B. halotolerans* KFD is very well adapted to date palm roots and familiar with the bayoud ecosystem. Indeed, several studies have shown that infected plants could recruit beneficial microbes to limit the propagation of phytopathogens (Berendsen et al., 2018; Rolfe et al., 2019; Gao et al., 2021). During this phenomenon described as "cry out for help", plants, through their root exudates, are thought to assemble protective microbes as a protective mechanism. This could explain the reason why *B. halotolerans* KFD was isolated from the bayoud-infected date palm rhizoplane. In the case that KFD was specifically recruited to protect date palm against Foa, its use for bayoud disease management agent could be impactful. However, further studies are required to validate this hypothesis, and on-field experiments are required to validate the biocontrol effect of *B. halotolerans* KFD and investigate the development of adequate formulations to facilitate dissemination strategies, which can be challenging.

5. Conclusion

In the frame of developing alternative solutions in the management of bayoud disease, our study investigated the potential of isolating, from the rhizosphere of date palm, microorganisms with high antifungal activity to combat the bayoud causal pathogen Foa. *B. halotolerans* KFD that we isolated from date palm showed interesting PGP and antifungal properties against Foa as well as a large antifungal spectrum against other plant pathogens. Moreover, it showed effective control of Foa in an *in vivo* greenhouse assay on date palm seedlings. The molecular characterization of isolate KFD showed that it belongs to *B. halotolerans*. To the best of our knowledge, our study is the first to isolate and describe the genomic features of a *B. halotolerans* strain from the rhizosphere of date palm and the first to report the antifungal activity of a *B. halotolerans* strain against *F. proliferatum*. In the genome of *B. halotolerans KFD* we identified genes encoding CAZymes that can degrade chitin and beta-glucan in fungal cell walls as well as different BGCs encoding for antifungal metabolites. The connective secretion of antifungal secondary metabolites and cell wall-degrading enzymes reported in *B. halotolerans* KFD reflects its ability to control the growth of Foa and other plant phytopathogenic fungi. The results we obtained show that *B. halotolerans* KFD could play a substantial role in managing bayoud disease and promoting the growth of date palms. Therefore, future perspective should be focused on the functional validation of KFD beneficial genes thought transcriptome analysis. Moreover, the transcriptome and defence-related enzyme analysis of challenged date palm should be studied to better understand the biocontrol mechanism of *B. halotolerans* KFD. On-field assays are also considered before proposing KFD as a bayoud management alternatives to date palm growers.

CRediT authorship contribution statement

Aliou Moussa Diouf: Writing – original draft, Validation, Methodology, Formal analysis, Conceptualization. **Abdou Lahat Mbaye:** Methodology. **Maimouna Deh:** Methodology. **Mustapha Barakate:** Writing – review & editing, Validation, Supervision. **Zineb Rchiad:** Writing – review & editing, Validation, Supervision.

Funding

This work was supported by Bayoud and AS79 projects funded by the OCP Foundation. A part of this work was also supported by the grant of PRIMA-SUSTEMICROP project (Section 2-2021).

Declaration of competing interest

The authors declare that they have no known competing financial interests or personal relationships that could have appeared to influence the work reported in this paper.

Acknowledgement

We would like to thank all the laboratory of the College of Agriculture and Environmental Sciences with a particular thanks to the Agro-Biosciences Division. We thank Pr. Mohammed Aziz El Houmaizi for helping to collect the sample from the Oasis.

Appendix A. Supplementary material

Supplementary data to this article can be found online at https://doi.org/10.1016/j.biocontrol.2025.105790.

References

Abdalla, M.Y., et al., 2000. Pathogenicity of toxigenic *fusarium proliferatum* from date palm in Saudi Arabia. *Plant Disease* 84 (3), 321–324. https://doi.org/10.1094/PDIS.2000.84.3.321.

Abouamama, S., et al., 2018. Pathogenicity and biological control of bayoud disease by *trichoderma longibrachiatum* and *artemisia herba-alba* essential oil. *J. Appl. Pharma. Sci.* 8 (4), 161–167. https://doi.org/10.7324/JAPS.2018.8423.

Almagro Armenteros, J.J., et al., 2019. SignalP 5.0 improves signal peptide predictions using deep neural networks. *Nat. Biotechnol.* 37 (4), 420–423. https://doi.org/10.1038/s41587-019-0036-z.

Ballantine, R.D., et al., 2023. Linearization of the brevicidine and laterocidine lipopeptides yields analogues that retain full antibacterial activity. *J. Med. Chem.* 66 (8), 6002–6009. https://doi.org/10.1021/ACS.JMEDCHEM.3C00308/SUPPL_FILE/JM3C00308_SI_002.CSV.

Barnawal, D., et al., 2017. ACC deaminase-containing plant growth-promoting rhizobacteria protect *Papaver somniferum* from downy mildew. *J. Appl. Microbiol.* 122 (5), 1286–1298. https://doi.org/10.1111/jam.13417.

Benzohra, I.E., Megateli, M. and Berdja, R. (2015) 'Bayoud disease of date palm in Algeria : History, epidemiology and integrated disease management', 14(7), pp. 542–550. Available at: Doi: 10.5897/AJBX2014.14292.

Berendsen, R.L., et al., 2018. Disease-induced assemblage of a plant-beneficial bacterial consortium. *The ISME J.* 12 (6), 1496–1507. https://doi.org/10.1038/s41396-018-0093-1.

Blake, C., Christensen, M.N., Kovács, Á.T., 2021. Molecular aspects of plant growth promotion and protection by Bacillus subtilis. *Mol. Plant-Microbe Int.* 34 (1), 15–25.

Boulahouat, S., et al., 2022. Critical evaluation of biocontrol ability of bayoud infected date palm phyllospheric *bacillus* spp. suggests that in vitro selection does not guarantee success in planta. *Agronomy* 12, 2403. https://doi.org/10.3390/agronomy12102403.

Ciufo, S., et al., 2018. Using average nucleotide identity to improve taxonomic assignments in prokaryotic genomes at the NCBI. *Int. J. System. Evolut. Microbiol.* 68 (7), 2386–2392. https://doi.org/10.1099/ijsem.0.002809.

Collinge, D.B., et al., 2022. Biological control of plant diseases – What has been achieved and what is the direction? Plant Pathol. 71 (5), 1024–1047. https://doi.org/10.1111/ppa.13555.

Correa, O. and Soria, M. (2010) 'Potential of Bacilli for Biocontrol and Its Exploitation in Sustainable Agriculture', in, pp. 197–209. Doi: 10.1007/978-3-642-13612-2_8.

Dihazi, A., et al., 2012a. Use of two bacteria for biological control of bayoud disease caused by Fusarium oxysporum in date palm (Phoenix dactylifera L) seedlings. Plant Physiol. Biochem. 55, 7–15. https://doi.org/10.1016/j.plaphy.2012.03.003.

Dihazi, A., et al., 2012b. Use of two bacteria for biological control of bayoud disease caused by Fusarium oxysporum in date palm (Phoenix dactylifera L) seedlings. Plant Physiol. Biochem. 55, 7–15. https://doi.org/10.1016/j.plaphy.2012.03.003.

Dixit, R., et al., 2016. Southern blight disease of tomato control by 1-aminocyclopropane-1-carboxylate (ACC) deaminase producing Paenibacillus lentimorbus B-30488. Plant Signaling Behavior. 11 (2). https://doi.org/10.1080/15592324.2015.1113363.

Donate-Correa, J., León-Barrios, M., Pérez-Galdona, R., 2005. Screening for plant growth-promoting rhizobacteria in Chamaecytisus proliferus (tagasaste), a forage tree-shrub legume endemic to the Canary Islands. Plant and Soil 266 (1), 261–272. https://doi.org/10.1007/s11104-005-0754-5.

Dworkin, M., Foster, J., 1958. Experiments with some microorganisms which utilize ethane and hydrogen. *J. Bacteriol.* 75 (5), 592–603.

Emms, D.M., Kelly, S., 2019. OrthoFinder: phylogenetic orthology inference for comparative genomics. Genome Biol. 20 (1), 238. https://doi.org/10.1186/s13059-019-1832-y.

Feng, Z., et al., 2022. Molecular characterization of a novel strain of *Bacillus halotolerans* protecting wheat from sheath blight disease caused by Rhi*zoctonia solani* Kühn. *Front. Plant Sci.* 13. https://doi.org/10.3389/fpls.2022.1019512.

Fu, L., et al., 2012. CD-HIT: accelerated for clustering the next-generation sequencing data. Bioinformatics 28 (23), 3150–3152. https://doi.org/10.1093/bioinformatics/bts565.

Gaderer, R., Seidl-Seiboth, V., Kappel, L., 2017. Chitin and N-acetylglucosamine metabolism in fungi-a complex machinery harnessed for the design of chitin-based high value products. *Curr. Biotechnol.* 6 (3), 178–193.

Gao, L., et al., 2017. Plipastatin and surfactin coproduction by Bacillus subtilis pB2-L and their effects on microorganisms. Antonie van Leeuwenhoek 110 (8), 1007–1018. https://doi.org/10.1007/s10482-017-0874-y.

Gao, M., et al., 2021. Disease-induced changes in plant microbiome assembly and functional adaptation. Microbiome 9 (1), 187. https://doi.org/10.1186/s40168-021-01138-2.

Ghorbanpour, M., et al., 2018. Mechanisms underlying the protective effects of beneficial fungi against plant diseases. *Biol. Control* 117, 147–157.

Gong, A.-D., et al., 2015. Antagonistic mechanism of iturin a and plipastatin a from bacillus amyloliquefaciens S76–3 from wheat spikes against fusarium graminearum. PLOS ONE 10 (2). https://doi.org/10.1371/journal.pone.0116871.

Gurevich, A., et al., 2013. QUAST: quality assessment tool for genome assemblies. Bioinformatics 29 (8), 1072–1075. https://doi.org/10.1093/bioinformatics/btt086.

Gwa, V.I., Ekefan, E.J., 2024. Microbial secondary metabolites and their roles in biocontrol of phytopathogens. Bioactive Microbial Metabolites 1–30. https://doi.org/10.1016/B978-0-443-18568-7.00007-0.

Haq, I.U., et al., 2024. Eco-smart biocontrol strategies utilizing potent microbes for sustainable management of phytopathogenic diseases. Biotechnol. Rep. 44. https://doi.org/10.1016/j.btre.2024.e00859.

Harwood, C.R., et al., 2018. Secondary metabolite production and the safety of industrially important members of the Bacillus subtilis group. FEMS Microbiol. Rev. 42 (6), 721–738. https://doi.org/10.1093/femsre/fuy028.

El Hassni, M., et al., 2007a. Biological control of bayoud disease in date palm: selection of microorganisms inhibiting the causal agent and inducing defense reactions. Environ. Experim. Botany 59 (2), 224–234. https://doi.org/10.1016/j.envexpbot.2005.12.008.

El Hassni, M., et al., 2007b. Biological control of bayoud disease in date palm: selection of microorganisms inhibiting the causal agent and inducing defense reactions. Environ. Experim. Botany 59 (2), 224–234. https://doi.org/10.1016/j.envexpbot.2005.12.008.

Khan, N., et al., 2018. Antifungal activity of bacillus species against fusarium and analysis of the potential mechanisms used in biocontrol. Front. Microbiol. 9. https://doi.org/10.3389/FMICB.2018.02363/BIBTEX.

Kiesewalter, H., et al., 2021. Genomic and chemical diversity of bacillus subtilis secondary metabolites against plant pathogenic fungi. mSystems 6 (1). https://doi.org/10.1128/msystems.00770-20.

Köhl, J., Kolnaar, R., Ravensberg, W.J., 2019. Mode of action of microbial biological control agents against plant diseases: relevance beyond efficacy. Front. Plant Sci. 10. https://doi.org/10.3389/fpls.2019.00845.

Koteshwara, A., 2021. Simple methods for the preparation of colloidal chitin, cell free supernatant and estimation of laminarinase. Bio-protocol 11 (19). https://doi.org/10.21769/BIOPROTOC.4176.

Li, S., et al., 2022. Biocontrol of wheat crown rot using *bacillus halotolerans* QTH8. Pathogens 11 (5). https://doi.org/10.3390/pathogens11050595.

Li, W., et al., 2020. Mediation of induced systemic resistance by the plant growth-promoting rhizobacteria *Bacillus pumilus* S2-3-2. *Mol. Biol. Rep.* 47 (11), 8429–8438.

Li, X., et al., 2025. Whole genome-sequence analysis of Bacillus subtilis strain KC14-1 with broad-spectrum antifungal activity. BMC Genomics 26 (1), 1–14. https://doi.org/10.1186/S12864-025-11227-3/TABLES/3.

Liu, G.H., et al., 2019. Genome-based reclassification of bacillus okuhidensis as a later heterotypic synonym of bacillus halodurans. Int. J. Syst. Evolut. Microbiol. 69 (11), 3599–3602. https://doi.org/10.1099/IJSEM.0.003666/CITE/REFWORKS.

Manni, M., et al., 2021. BUSCO: assessing genomic data quality and beyond. Current Protocols 1 (12). https://doi.org/10.1002/cpz1.323.

El Modafar, C., 2010. Mechanisms of date palm resistance to Bayoud disease: current state of knowledge and research prospects. Physiol. Mol. Plant Pathol. 74 (5–6), 287–294. https://doi.org/10.1016/J.PMPP.2010.06.008.

Pan, D., et al., 2023. Research progress of lytic chitin monooxygenase and its utilization in chitin resource fermentation transformation. Fermentation 9 (8). https://doi.org/10.3390/fermentation9080754.

Prjibelski, A., et al., 2020. Using SPAdes De Novo Assembler. Curr. Prot. Bioinform. 70 (1). https://doi.org/10.1002/cpbi.102.

Rafiqi, M., et al., 2022. Profile of the in silico secretome of the palm dieback pathogen, fusarium oxysporum f. sp. albedinis, a fungus that puts natural oases at risk. PLOS ONE 17 (5), e0260830. https://doi.org/10.1371/journal.pone.0260830.

Rolfe, S.A., Griffiths, J., Ton, J., 2019. Crying out for help with root exudates: adaptive mechanisms by which stressed plants assemble health-promoting soil microbiomes. Curr. Opin. Microbiol. 49, 73–82. https://doi.org/10.1016/J.MIB.2019.10.003.

Saima, et al., 2013. Isolation of novel chitinolytic bacteria and production optimization of extracellular chitinase. J. Genetic Eng. Biotechnol. 11 (1), 39–46. https://doi.org/10.1016/J.JGEB.2013.03.001.

Salazar, B., et al., 2023. *Bacillus* spp. as bio-factories for antifungal secondary metabolites: Innovation beyond whole organism formulations. *Micro. Ecol.* 86 (1), 1–24.

Samaras, A., et al., 2021. *Bacillus subtilis* MBI600 promotes growth of tomato plants and induces systemic resistance contributing to the control of soilborne pathogens. *Plants* 10 (6), 1113.

Sansinenea, E. (2019) '*Bacillus* spp.: As plant growth-promoting bacteria', *Secondary metabolites of plant growth promoting rhizomicroorganisms: Discovery and applications*, pp. 225–237.

Schwyn, B., Neilands, J., 1987. Universal chemical assay for the detection and determination of siderophores. *Anal. Biochem.* 160 (1), 47–56.

Seemann, T., 2014. Prokka: rapid prokaryotic genome annotation. Bioinformatics 30 (14), 2068–2069. https://doi.org/10.1093/bioinformatics/btu153.

Shafi, J., Tian, H., Ji, M., 2017. Bacillus species as versatile weapons for plant pathogens: a review. Biotechnol. Biotechnol. Equip. 31 (3), 446–459. https://doi.org/10.1080/13102818.2017.1286950.

Slama, H Ben, et al., 2019. Screening for fusarium antagonistic bacteria from contrasting niches designated the endophyte bacillus halotolerans as plant warden against fusarium. Front. Microbiol. 9. https://doi.org/10.3389/fmicb.2018.03236.

Thomloudi, E.-E., et al., 2021. Genomic and metabolomic insights into secondary metabolites of the novel *bacillus halotolerans* Hil4, an endophyte with promising antagonistic activity against gray mold and plant growth promoting potential. *Microorganisms* 9 (12). https://doi.org/10.3390/microorganisms9122508.

Tran, C., et al., 2022. Antimicrobial *bacillus*: metabolites and their mode of action. *Antibiotics* 11 (1), 88.

Tsalgatidou, P.C., et al., 2022. Integrated genomic and metabolomic analysis illuminates key secreted metabolites produced by the novel endophyte bacillus halotolerans cal. l.30 involved in diverse biological control activities. Microorganisms 10 (2). https://doi.org/10.3390/microorganisms10020399.

Tuyen, D.T., et al., 2023. Antifungal activity of secondary metabolites purified from Bacillus subtilis isolated in Vietnam and evaluated on in vitro and in vivo models. Int. Biodeteri. & Biodegrad. 179. https://doi.org/10.1016/j.ibiod.2022.105558.

Ulrich, N., et al., 2018. Experimental studies addressing the longevity of Bacillus subtilis spores - the first data from a 500-year experiment. PloS one 13 (12), e0208425. https://doi.org/10.1371/journal.pone.0208425.

Wang, F., et al., 2021. Biocontrol ability and action mechanism of Bacillus halotolerans against Botrytis cinerea causing grey mould in postharvest strawberry fruit. Postharvest Biol. Technol. 174. https://doi.org/10.1016/j.postharvbio.2020.111456.

Wang, Y., et al., 2024. Whole-genome analysis revealed the growth-promoting and biological control mechanism of the endophytic bacterial strain Bacillus halotolerans Q2H2, with strong antagonistic activity in potato plants. Front. Microbiol. 14. https://doi.org/10.3389/fmicb.2023.1287921.

Yang, F., et al., 2023. Genome sequencing and analysis of Bacillus velezensis VJH504 reveal biocontrol mechanism against cucumber Fusarium wilt. Front. Microbiol. 14, 1279695. https://doi.org/10.3389/FMICB.2023.1279695/BIBTEX.

Yang, P., et al., 2023. *Bacillus proteolyticus* OSUB18 triggers induced systemic resistance against bacterial and fungal pathogens in Arabidopsis. *Front. Plant Sci.* 14, 1078100.

Yi, Hu, et al., 2025. Research and development progress and application challenges of bacterial biocontrol agents. Front. Agri. 2 (1), 1–8. https://doi.org/10.71465/FA34.

Zhu, J., et al., 2020. Biocontrol potential of Bacillus subtilis IBFCBF-4 against Fusarium wilt of watermelon. J. Plant Pathol. 102 (2), 433–441. https://doi.org/10.1007/s42161-019-00457-6.